Chapter 8
MPC of State-Space Benchmark Wiener Processes

Please cite the book:
Maciej Ławryńczuk: Nonlinear Predictive Control Using Wiener Models: Computationally Efficient Approaches for Polynomial and Neural Structures. Studies in Systems, Decision and Control, vol. 389, Springer, Cham, 2022.

Abstract This Chapter thoroughly discusses implementation details and simulation results of various MPC algorithms introduced in the previous Chapter applied to state-space benchmark processes. One SISO process and two MIMO ones are considered: the first MIMO benchmark has two inputs and two outputs, the second one has as many as ten inputs and two outputs. Efficiency of different methods allowing for offset-free control is considered. All algorithms are compared in terms of control quality and computational time.

8.1 The State-Space SISO Process

8.1.1 Description of the State-Space SISO Process

Let us consider the SISO process which is a state-space representation of the Wiener system introduced in Chapter 4.2. The corresponding matrices of the model (2.84)-(2.85) are

$$\boldsymbol{A} = \begin{bmatrix} 1.4138 & -6.0650 \times 10^{-1} \\ 1 & 0 \end{bmatrix}, \ \boldsymbol{B} = \begin{bmatrix} 1 \\ 0 \end{bmatrix}, \ \boldsymbol{C} = \begin{bmatrix} 1.0440 \times 10^{-1} & 8.8300 \times 10^{-2} \end{bmatrix} \tag{8.1}$$

The nonlinear static block is the same as in the input-output description (Eq. (4.4)). The steady-state characteristic $y(u)$ of the whole Wiener system is depicted in Fig. 4.1.

8.1.2 Implementation of MPC Algorithms for the State-Space SISO Process

The following MPC algorithms are compared:

1. The classical LMPC algorithm based on a linear model (three example models, obtained for different operating points, are considered).
2. The MPC-SSL and MPC-NPSL algorithms.
3. The MPC-NPLT1, MPC-NPLT2 and MPC-NPLPT algorithms.
4. The MPC-NO algorithm.

In all listed algorithms, the discussed offset-free prediction method is used. Additionally, two MPC-NO algorithms with the classical augmented state disturbance model are considered:

1. The MPC-NOaug1 algorithm: the disturbance estimation is placed in the first state equation.
2. The MPC-NOaug2 algorithm: the disturbance estimation is placed in the second state equation.

In general, all universal equations presented in Chapter 7 are used. Additional specific relations that depend on the static parts of the model are the same as for the input-output version of the process (Eqs. (4.5)-(4.8)).

8.1.3 MPC of the State-Space SISO Process

Parameters of all compared MPC algorithms are the same as in the input-output SISO process case (Chapter 4.2): $N = 10$, $N_u = 3$, $\lambda = 0.25$, the constraints imposed on the manipulated variable are: $u^{min} = -2.5$, $u^{max} = 2.5$. Similarly to the input-output SISO benchmark, for the state-space one, we also consider two cases: no modelling errors and no disturbances, whereas in the second part, robustness to external disturbances is evaluated. In order to demonstrate advantages of the prediction model used for offset-free control, a comparison with the method using the classical augmented state disturbance model is made.

In the first part of simulations, the model is perfect (no modelling errors) and the process is not affected by any disturbances. Simulation results of the LMPC algorithm are given in Fig. 8.1, three versions of the algorithm are verified for linear models from three different operating points (the same as in the input-output SISO process case). Unfortunately, due to process nonlinearity, the LMPC algorithm does not lead to good control quality. It is interesting to note that the algorithm results in different trajectories in comparison with those obtained for the input-output SISO case depicted in Fig. 4.2.

Next, we consider simulation results of the MPC-NPSL and MPC-SSL algorithms. They are shown in Fig. 8.2, the trajectories obtained when the reference

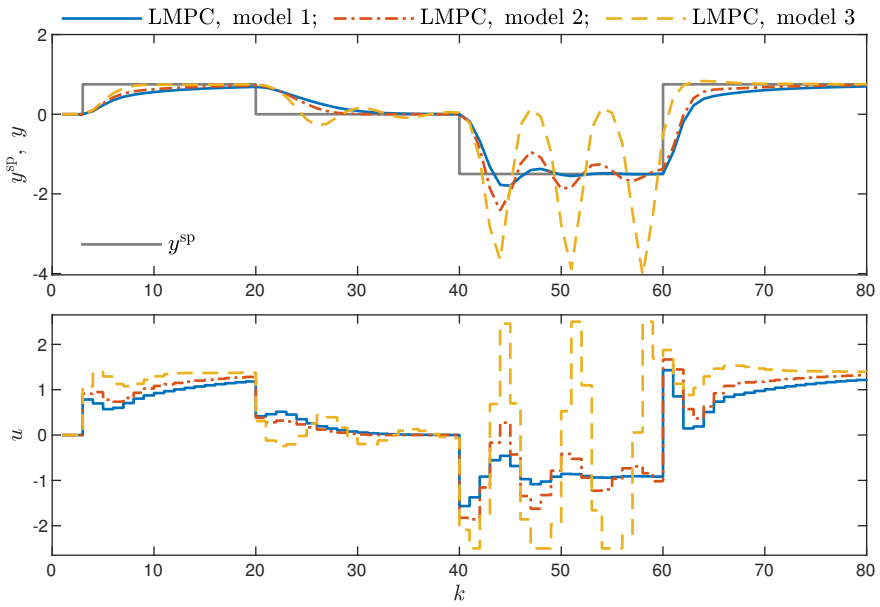

Fig. 8.1 The state-space SISO process: simulation results of the linear LMPC algorithm based on different models, obtained for different operating points

MPC-NO scheme is used are also given for comparison. The MPC-NPSL scheme gives good control. Depending on the operating point, the MPC-SSL algorithm is slightly slower or it gives larger overshoot. When compared with the results obtained for the input-output SISO case and depicted in Fig. 4.3, it is interesting to note that the MPC-SSL scheme in both cases gives similar trajectories, but the differences are not significant. The MPC-NPSL and MPC-NO schemes for both model representations give the same results.

Simulation results of the MPC-NPLPT, MPC-NPLT1 and MPC-NPLT2 algorithms are not shown since the results for the state-space SISO process are the same as their versions in the input-output case shown in Fig. 4.5. Let us recall that the algorithms with one on-line trajectory linearisation at each sampling instant are better than the MPC schemes with model linearisation and the MPC-NPLPT method gives practically the same results as the MPC-NO approach.

All considered MPC algorithms are compared in Table 8.1 in terms of the performance criteria E_2, $E_{\text{MPC-NO}}$, the number of internal iterations necessary in the MPC-NPLPT algorithm and the calculation time. Control accuracy of LMPC and MPC-SSL approaches are different in comparison with the input-output SISO case (Table 4.1); all other algorithms give the same results. As far as the computational time is concerned, as always, the more advanced the algorithm, the longer the time required. It is important that the MPC algorithms with model or trajectory lineari-

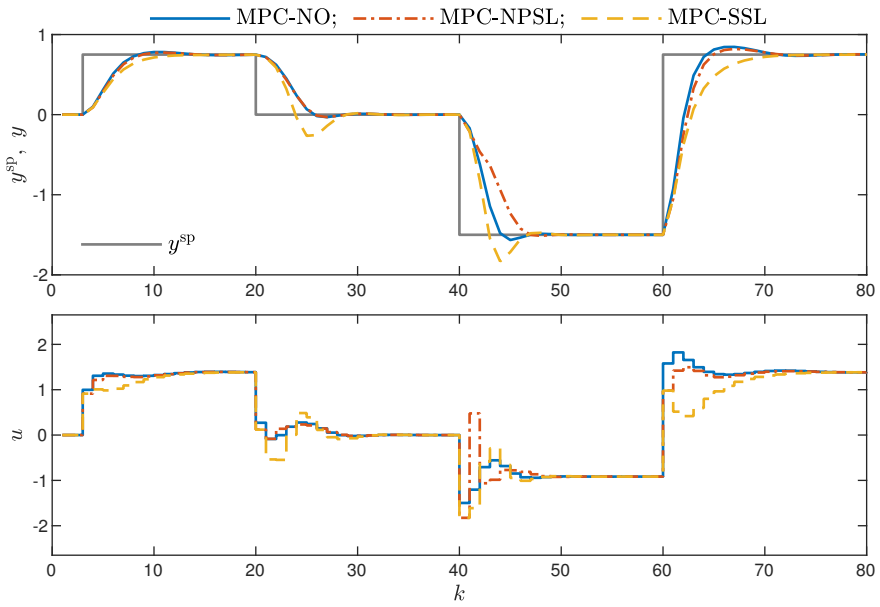

Fig. 8.2 The state-space SISO process: simulation results of the MPC-NO, MPC-NPSL and MPC-SSL algorithms

sation require only a fraction of the calculation time necessary in the MPC-NO scheme.

Furthermore, it is interesting to analyse the relative computational time of all tested MPC algorithms for both input-output and state-space representations for the SISO process, for different values of the control horizon. The results are given in Table 8.2. All results are scaled in such a way that the computational time for the MPC-NO algorithm based on the state-space Wiener model and for default horizons ($N = 10$, $N_u = 3$), corresponds to 100%. Of course, the results depend on software implementation of the algorithms, but, in our case, it turns out that the MPC-NO algorithm for the state-space version of the process needs more calculation time than its version for the input-output domain. It explains why the computation times of MPC algorithms with linearisation (in relation to the computation time of the MPC-NO scheme) are longer in Table 4.1 than in Table 8.1. On the other hand, relative relations of the calculation time of the consecutive MPC algorithms are very similar in the case of both model representations, i.e. simple MPC-SSL and MPC-NPSL schemes need less time than advanced MPC-NPLT and MPC-NPLPT methods.

In the second part of simulations we assume that the set-point is constant ($y^{sp}(k) = 0 \; \forall \; k$), but the process is affected by disturbances. In all MPC algorithms, the ideal

Table 8.1 The state-space SISO process: comparison of all considered MPC algorithms in terms of the control performance criteria (E_2 and $E_{\text{MPC-NO}}$), the sum of internal iterations (SII) and the calculation time

Algorithm	E_2	$E_{\text{MPC-NO}}$	SII	Calculation time (%)
LMPC, model 1	1.8429×10^{1}	1.7121	–	14.3
LMPC, model 2	1.7659×10^{1}	3.0966	–	14.2
LMPC, model 3	4.5266×10^{1}	4.1417×10^{1}	–	14.3
MPC-SSL	1.7928×10^{1}	1.3882	–	19.2
MPC-NPSL	1.8641×10^{1}	8.0533×10^{-1}	–	21.6
MPC-NPLT1	1.6917×10^{1}	1.6184×10^{-1}	–	19.0
MPC-NPLT2	1.7006×10^{1}	2.1282×10^{-1}	–	19.0
MPC-NPLPT, $\delta = 10$	1.6968×10^{1}	2.1156×10^{-1}	79	19.5
MPC-NPLPT, $\delta = 1$	1.6363×10^{1}	4.7067×10^{-3}	95	21.7
MPC-NPLPT, $\delta = 10^{-1}$	1.6513×10^{1}	2.6107×10^{-5}	108	23.3
MPC-NPLPT, $\delta = 10^{-2}$	1.6524×10^{1}	5.3491×10^{-7}	123	24.9
MPC-NPLPT, $\delta = 10^{-3}$	1.6523×10^{1}	3.4081×10^{-7}	134	26.5
MPC-NPLPT, $\delta = 10^{-4}$	1.6523×10^{1}	3.4170×10^{-7}	146	28.4
MPC-NPLPT, $\delta = 10^{-5}$	1.6523×10^{1}	4.4880×10^{-7}	155	29.1
MPC-NO	1.6524×10^{1}	–	–	100.0

Table 8.2 The input-output SISO process vs. the state-space SISO process: comparison of all considered MPC algorithms in terms of the calculation time (%) for different control horizons, $N = 10$

Algorithm	Model	$N_u = 1$	$N_u = 2$	$N_u = 3$	$N_u = 4$	$N_u = 5$	$N_u = 10$
LMPC	Input-output	13.7	14.1	13.7	14.2	14.3	14.8
MPC-SSL		14.1	14.8	14.5	14.9	15.0	15.6
MPC-NPSL		14.2	14.9	14.5	15.0	15.2	15.6
MPC-NPLT1		14.6	15.6	16.0	15.9	16.1	16.5
MPC-NPLPT, $\delta = 10$		15.5	16.1	15.8	16.3	16.6	17.0
MPC-NPLPT, $\delta = 1$		16.6	18.3	17.3	18.0	18.1	18.9
MPC-NPLPT, $\delta = 10^{-1}$		18.1	18.7	18.2	18.8	19.2	20.3
MPC-NPLPT, $\delta = 10^{-2}$		19.2	19.7	19.3	20.4	20.3	21.3
MPC-NPLPT, $\delta = 10^{-3}$		20.4	20.8	20.4	21.3	21.5	22.6
MPC-NPLPT, $\delta = 10^{-4}$		21.5	21.7	21.6	22.5	22.7	23.9
MPC-NPLPT, $\delta = 10^{-5}$		22.2	22.7	22.0	23.3	23.6	25.1
MPC-NO		25.2	32.7	37.4	46.1	48.0	63.6
LMPC	State-space	13.6	14.2	14.3	14.4	14.4	15.0
MPC-SSL		18.4	19.0	19.2	19.2	19.6	19.9
MPC-NPSL		20.7	21.5	21.6	21.5	21.9	22.2
MPC-NPLT1		17.7	18.7	19.0	19.0	19.1	19.8
MPC-NPLPT, $\delta = 10$		18.7	19.1	19.5	19.5	19.5	20.8
MPC-NPLPT, $\delta = 1$		20.3	21.3	21.7	22.0	21.7	22.5
MPC-NPLPT, $\delta = 10^{-1}$		22.5	22.8	23.3	23.4	23.4	24.2
MPC-NPLPT, $\delta = 10^{-2}$		24.2	24.5	24.9	25.4	25.2	26.1
MPC-NPLPT, $\delta = 10^{-3}$		26.3	26.1	26.5	26.8	27.0	28.2
MPC-NPLPT, $\delta = 10^{-4}$		28.0	27.6	28.4	28.6	28.8	30.0
MPC-NPLPT, $\delta = 10^{-5}$		28.6	29.1	29.1	29.6	29.9	31.1
MPC-NO		47.0	71.7	100.0	125.2	146.4	243.6

Wiener model is used, whereas the simulated process is

$$\begin{bmatrix} x_1(k+1) \\ x_2(k+1) \end{bmatrix} = \boldsymbol{A} \begin{bmatrix} x_1(k) \\ x_2(k) \end{bmatrix} + \begin{bmatrix} d_1^{\mathrm{x}}(k) \\ d_2^{\mathrm{x}}(k) \end{bmatrix} + \boldsymbol{B}(u(k) + d^{\mathrm{u}}(k)) \tag{8.2}$$

$$y(k) = g(\boldsymbol{C}x(k)) + d^{\mathrm{y}}(k) \tag{8.3}$$

The disturbances are

$$\begin{aligned} d_1^{\mathrm{x}}(k) &= -0.2H(k-3), & d_2^{\mathrm{x}}(k) &= 0.3H(k-20) \\ d^{\mathrm{u}}(k) &= 0.5H(k-60), & d^{\mathrm{y}}(k) &= 0.4H(k-40) \end{aligned} \tag{8.4}$$

where the Heaviside step function is

$$H(k) = \begin{cases} 0 & \text{if } k < 0 \\ 1 & \text{if } k \geq 0 \end{cases} \tag{8.5}$$

In the state-space domain, we not only consider the unmeasured disturbance that acts on the process output, as it is the case in the input-output approach, but we also take into account state and input disturbances.

Simulation results of two simple MPC algorithms with on-line model linearisation, i.e. the MPC-SSL and MPC-NPSL strategies, are presented in Fig. 8.3, the trajectories obtained in the MPC-NO one are given for reference. Although the MPC-NPSL algorithm works correctly in set-point tracking (and the disturbance-free case) as depicted in Fig. 8.2, for disturbance compensation the default parameter $\lambda = 0.25$ leads to very poor performance and must be increased to $\lambda = 0.5$. The MPC-SSL scheme works correctly, but there are some differences from the ideal trajectory possible when the MPC-NO scheme is used.

Fig. 8.4 compares the results obtained for three MPC algorithms with on-line trajectory linearisation, i.e. the MPC-NPLT1, MPC-NPLT2 and MPC-NPLPT strategies, the trajectories of the MPC-NO approach are also given for reference. Two observations may be made. Firstly, the MPC-NPLPT algorithm gives the same trajectory as the MPC-NO one, which is also observed in the set-point tracking task without disturbances (Table 8.1). Secondly, in the case of the disturbances, the algorithms with one linearisation at each sampling instant, i.e. the MPC-NPLT1 and MPC-NPLT2 ones, give different trajectories than those of the MPC-NO algorithm, whereas very small differences are observed in the set-point tracking task. Fig. 8.5 compares the real and estimated state trajectories in the MPC-NPLPT algorithm. It is interesting to notice significant differences between them. Nevertheless, thanks to using the discussed prediction and disturbance model, offset-free control is assured.

Fig. 8.6 compares performance of the MPC-NPLPT scheme and two versions of the MPC-NO algorithms with the augmented state disturbance model, i.e. MPC-

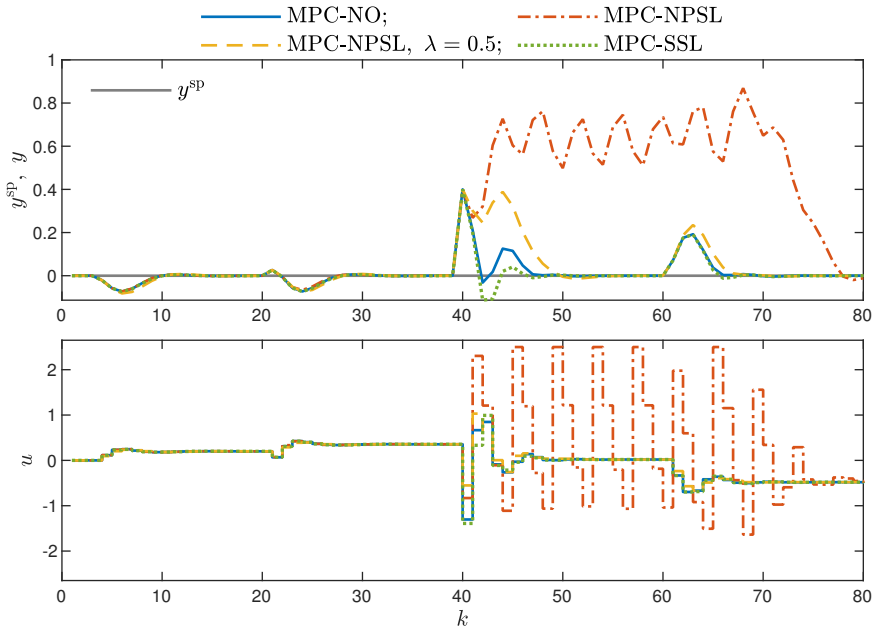

Fig. 8.3 The state-space SISO process (the set-point is constant, the unmeasured disturbances act on the process): simulation results of the MPC-NO, MPC-NPSL and MPC-SSL algorithms

Table 8.3 The state-space SISO process (the unmeasured disturbances act on the process): comparison of all considered MPC algorithms in terms of the control performance criteria (E_2 and $E_{\text{MPC-NO}}$), the sum of internal iterations (SII) and the calculation time

Algorithm	E_2	$E_{\text{MPC-NO}}$	SII	Calculation time (%)
LMPC, model 1	4.2260×10^{-1}	5.2117×10^{-2}	–	15.4
LMPC, model 2	3.8654×10^{-1}	6.5496×10^{-2}	–	15.3
LMPC, model 3	3.0833	2.9543	–	15.3
MPC-SSL	3.4180×10^{-1}	4.1471×10^{-2}	–	20.7
MPC-NPSL	1.3918×10^{1}	1.2560×10^{1}	–	22.9
MPC-NPSL, $\lambda = 0.5$	9.1647×10^{-1}	3.5257×10^{-1}	–	23.1
MPC-NPLT1	3.3592×10^{-1}	2.6668×10^{-2}	–	20.5
MPC-NPLT2	4.9184×10^{-1}	3.2912×10^{-1}	–	20.8
MPC-NPLPT, $\delta = 10$	4.9184×10^{-1}	3.2912×10^{-1}	79	21.1
MPC-NPLPT, $\delta = 1$	4.9184×10^{-1}	3.2912×10^{-1}	79	21.3
MPC-NPLPT, $\delta = 10^{-1}$	3.5118×10^{-1}	5.1177×10^{-4}	87	22.6
MPC-NPLPT, $\delta = 10^{-2}$	3.5129×10^{-1}	8.1146×10^{-5}	102	25.1
MPC-NPLPT, $\delta = 10^{-3}$	3.5411×10^{-1}	2.1422×10^{-5}	118	26.9
MPC-NPLPT, $\delta = 10^{-4}$	3.5301×10^{-1}	2.1185×10^{-6}	122	28.0
MPC-NPLPT, $\delta = 10^{-5}$	3.5311×10^{-1}	2.0078×10^{-6}	145	30.5
MPC-NO	3.5336×10^{-1}	–	–	100.0
MPC-NOaug1	4.4009×10^{-1}	3.5042×10^{-2}	–	121.3
MPC-NOaug2	5.8624×10^{-1}	1.3717×10^{-1}	–	118.6

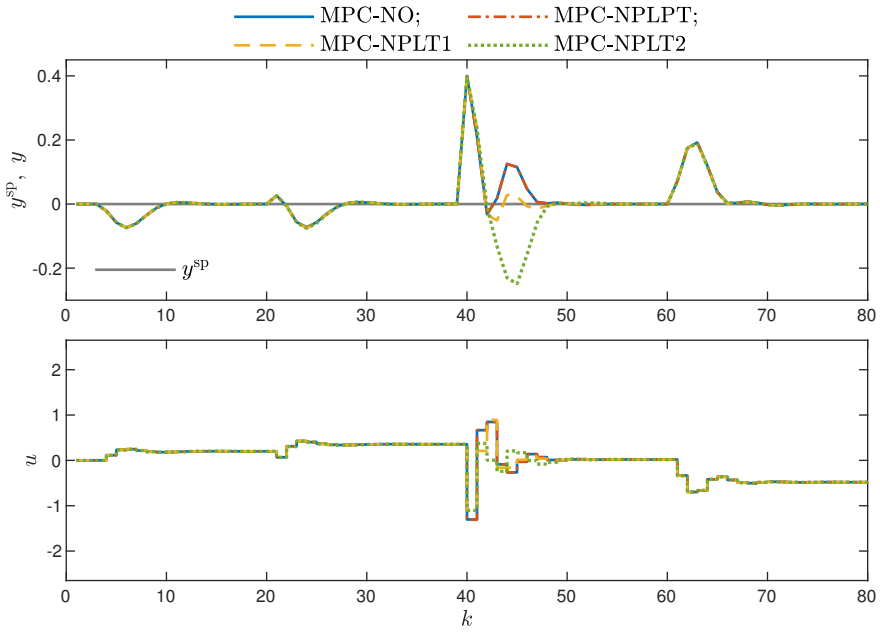

Fig. 8.4 The state-space SISO process (the set-point is constant, the unmeasured disturbances act on the process): simulation results of the MPC-NO, MPC-NPLPT, MPC-NPLT1 and MPC-NPLT2 algorithms

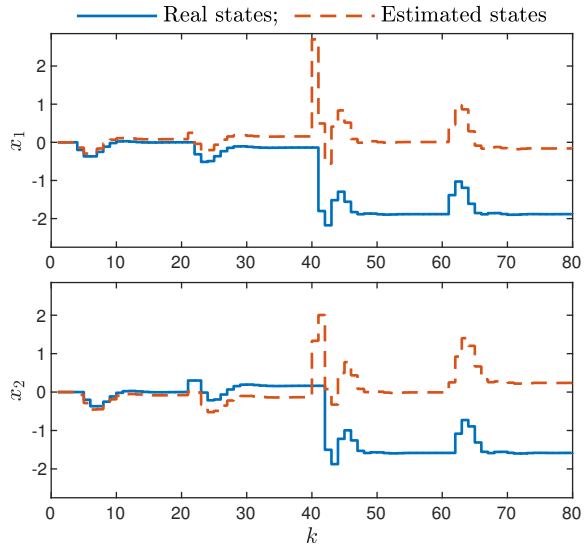

Fig. 8.5 The state-space SISO process (the set-point is constant, the unmeasured disturbances act on the process): the real vs. estimated state trajectories in the MPC-NPLPT algorithm

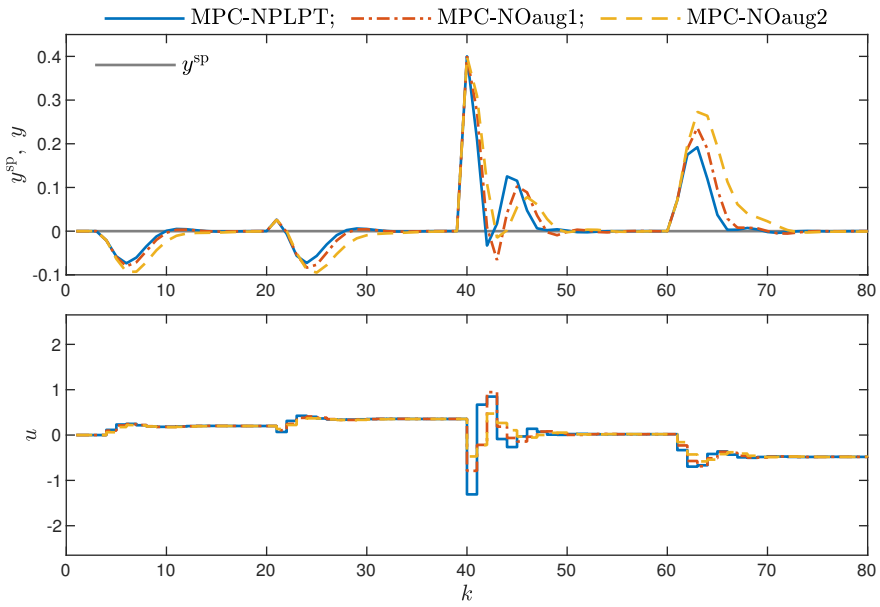

Fig. 8.6 The state-space SISO process (the set-point is constant, the unmeasured disturbances act on the process): simulation results of the MPC-NPLPT and two versions of the MPC-NOaug algorithms

NOaug1 and MPC-NOaug2. Although the MPC-NOaug1 scheme is faster than the MPC-NOaug2 one, the discussed MPC-NPLPT algorithm is the fastest one for each disturbance step. The obtained result corresponds with the general recommendations for the augmented state approach, i.e. the disturbance should be placed in the same equation in which the manipulated variable is present. The process matrix $\boldsymbol{B}$ (Eq. (8.1)) indicates that the disturbance should be placed in the first state equation.

All above observations are confirmed by numerical values of the performance criteria, E_2 and $E_{\text{MPC-NO}}$, detailed in Table 8.3. Similarly to the set-point tracking case (Table 8.1), the calculation time of the discussed MPC algorithms with linearisation is only a fraction of that necessary in the MPC-NO one.

8.2 The State-Space MIMO Process A with Two Inputs and Two Outputs: Model I

8.2.1 Description of the State-Space MIMO Process A

Let us consider the process which is a state-space representation of the MIMO Wiener system A introduced in Chapter 4.4. The corresponding matrices of the

model (2.84)-(2.85) are

$$\boldsymbol{A} = \begin{bmatrix} 0 & -7.3576 \times 10^{-1} & 0 & 0 \\ 5 \times 10^{-1} & 1.2131 & 0 & 0 \\ 0 & 0 & 0 & -4.3460 \times 10^{-1} \\ 0 & 0 & 1 & 1.3231 \end{bmatrix}, \tag{8.6}$$

$$\boldsymbol{B} = \begin{bmatrix} 5.1691 \times 10^{-1} & 1.0338 \times 10^{-1} \\ 3.6082 \times 10^{-1} & 7.2163 \times 10^{-2} \\ 3.8455 \times 10^{-2} & 4.8069 \times 10^{-1} \\ 5.0774 \times 10^{-2} & 6.3467 \times 10^{-1} \end{bmatrix}, \ \boldsymbol{C} = \begin{bmatrix} 0 & 5 \times 10^{-1} & 0 & 0 \\ 0 & 0 & 0 & 5 \times 10^{-1} \end{bmatrix} \tag{8.7}$$

The nonlinear static blocks (Eq. 2.14) are the same as in the input-output description (Eqs. (4.14)-(4.15)). The steady-state characteristics $y_1(u_1, u_2)$ and $y_2(u_1, u_2)$ of the whole Wiener system are depicted in Fig. 4.26.

8.2.2 Implementation of MPC Algorithms for the State-Space MIMO Process A

The following MPC algorithms are compared:

1. The classical LMPC algorithm based on a linear model (three example models, obtained for different operating points, are considered).
2. The MPC-SSL and MPC-NPSL algorithms.
3. The MPC-NPLT1, MPC-NPLT2 and MPC-NPLPT algorithms.
4. The MPC-NO algorithm.

In all listed algorithms, the discussed offset-free prediction method is used. Additionally, the MPC-NOaug algorithm with the classical augmented state disturbance model is considered. The additional disturbances are added to the manipulated variables (the best disturbance location in the model used).

In general, all universal equations presented in Chapter 7 are used. Additional specific relations that depend on the static parts of the model are the same as for the input-output version of the process (Eqs. (4.16)-(4.23)).

8.2.3 MPC of the State-Space MIMO Process A

Parameters of all compared MPC algorithms are the same as in the input-output MIMO process A case (Chapter 4.4): $N = 10$, $N_\mathrm{u} = 3$, $\mu_{p,1} = 1$ and $\mu_{p,2} = 5$ for $p = 1, \ldots, N$, $\lambda_{p,1} = \lambda_{p,2} = 0.5$ for $p = 0, \ldots, N_\mathrm{u} - 1$, constraints imposed on the manipulated variables are: $u_1^{\min} = u_2^{\min} = -1.5$, $u_1^{\max} = u_2^{\max} = 1.5$.

In the first part of simulations, the model is perfect and the process is not affected by any disturbances. Simulation results of the LMPC algorithm are given in Fig. 8.7,